Spin Echo Hemodynamic Impulse Response at 7 T

J. C. Siero[1,2], N. F. Ramsey[1], J. M. Hoogduin[1,2], P. R. Luijten[2], and N. Petridou[1,2]
[1]Rudolf Magnus Institute, University Medical Center Utrecht, Utrecht, Netherlands, [2]Radiology, University Medical Center Utrecht, Utrecht, Netherlands

Introduction

Understanding the mechanism of neurovascular coupling underlying the BOLD fMRI signal is contingent on the accurate spatial and temporal characterization of the hemodynamic impulse response (HIR), linked specifically to the microvasculature (capillary bed). At high field strength (≥7T), the gradient-echo (GE) HIR can differ across cortical depth [1,2], suggesting that voxels deeper in gray matter can more closely reflect the HIR of the microvasculature. However, GE BOLD can contain confounding contributions from the macrovasculature that drains toward the cortical surface, even at high field strength [3]. Alternatively, spin-echo (SE) BOLD at high field is more specific to the microvasculature, but sensitivity is low compared to GE BOLD [4] making it difficult to estimate the HIR. Here we obtained the SE HIR at 7T using a 16-channel surface coil for improved SNR [5], very short visual stimuli and high temporal resolution. The SE HIR was compared to GE HIR obtained near the pial surface and in deeper gray matter.

Materials and Methods

Data acquisition: Subjects were scanned on a Philips 7T system with a 16-channel surface coil [5]. SE functional data was obtained using a multislice single-shot SE-EPI acquisition with: TR/TE=880/55ms, FA=125°, SENSE factor=2, isotropic voxel size=2mm^3, FOV=195×180mm^2, and 5 coronal slices covering primary visual cortex V1. GE functional data were obtained using a multislice single-shot GE-EPI acquisition with: TR/TE=880/27ms, FA=70°, SENSE factor=3, isotropic voxel size=1mm^3, FOV=125×121 mm^2, and 7 coronal slices covering the same central area as the SE scan. 3rd order image based shimming on the FOV of the functional scans after brain extraction using BET [6]. A high resolution, 0.5mm^3 isotropic, T_2^*w scan was acquired as an anatomical reference. Cardiac and respiratory data were recorded during all scans. *Functional Paradigm:* For both GE and SE the functional scan consisted of four parts; i) 31s baseline period, ii) 463s event-related (ER) part, iii) 31s baseline period and, iv) 111s block design (localizer) part with off/on periods=15.8/15.8s (uniform gray screen / 8Hz reversing checkerboard). The event train for the ER part was generated with interstimulus intervals (ISI) taken from an exponential distribution between 2.9s and 19.6s (mean ISI=8.14s) [7]. A total of 61 stimuli were presented with stimulus duration of 250ms. Stimulus onset was uniformly jittered relative to the TR, yielding a sub-TR temporal resolution of 220ms. All conditions included a central red fixation point. *Data processing:* The functional scans were motion corrected, corrected for cardiac and respiratory fluctuations and linear trend [8, 9]. The localizer part was processed using FEAT: high pass filtering, slice timing correction, and no spatial smoothing, Z threshold=3.0 [10]. The largest significant cluster in V1 (cluster P threshold = 0.05, corrected) was selected and used as a region of interest for the ER-fMRI analysis. Large veins (and extravascular space) were identified based on their low intensity on high-res T2*w scan, and excluded from the GE data. Estimation of the HIR was done by means of conjugate gradients for deconvolution [11] after normalization by the baseline (mean of the two baseline periods), and 8-fold Fourier interpolation. Next, for every HIR we computed the time-to-peak (TTP), after slice timing correction, full-width at half maximum (FWHM) and percent signal change (PSC). For the GE data, for each HIR the distance to the cortical surface was estimated where the cortical surface was delineated manually on the high-res T2*w image after coregistration to the GE data (Fig1 inset, green line). Next, the distance was divided in three sections; 0 – 1 mm, 1 – 2 mm and 2 – 3 and the average HIR and TTP, FWHM, PSC was computed for every section.

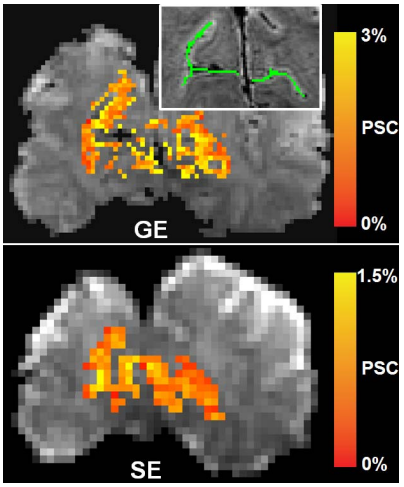

Figure 1: GE and SE percent signal change (PSC) maps of the estimate HIRs

Results

Fig1 shows the PSC maps for GE (top) and SE (bottom) for one representative subject. Smaller signal changes are evident for the SE responses. Fig2 shows the GE HIRs (average HIR for each cortical depth section in V1) and SE HIRs (average HIR of V1) for the same subject. Fig2 (right) shows the normalized HIRs to illustrate the differences in TTP and FWHM. For GE HIRs in deeper gray matter (1–3mm from the cortical surface) TTP and FWHM are 3.08s and 3.8s, respectively. For the SE HIR 3.08s and 2.8s, respectively. Also, the GE HIRs near the pial surface (0–1mm) show increased TTP (3.52s) and FWHM (4.18s) as compared to deeper gray matter GE HIRs and SE HIRs.

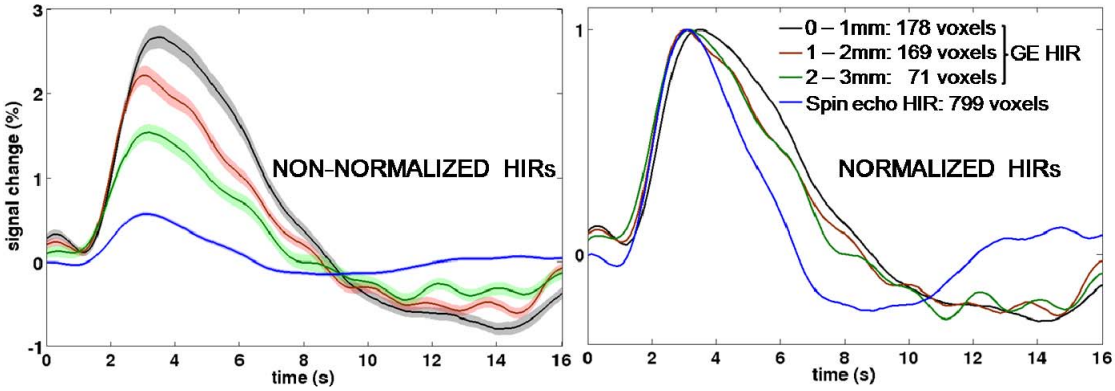

Figure 2: GE HIRs (black, red and green) across cortical depth in V1 and the SE HIR (blue) for V1. Shaded areas are SEM.

Discussion

Here we show that at 7 T the SE HIR can be accurately measured with high temporal resolution using very short (250ms) visual stimuli in an event-related paradigm. Initial results suggest that the TTP of SE HIR matches that of deeper gray matter GE HIR but not of the pial surface GE HIR. Also, the FWHM for the SE HIR are markedly shorter and differ from all GE HIRs in gray matter. Considering the specificity of SE to the microvasculature, the observed increased FWHM for GE HIRs in deeper gray matter are potentially caused by blood flow and/or pooling in postcapillary venuoles and intracortical vessels. However, the similarity in TTP between SE and GE HIR indicates that the earlier part of GE HIRs in deeper gray matter is less affected by confounding contributions from the macrovasculature. The SE HIR can lead to new insights to the factors that contribute to the GE HIR and the mechanisms underlying neurovascular coupling.

This project was funded by the Braingain consortium of the Netherlands

References

[1] Silva AC. et al PNAS(99) 2002, [2] Tian P. et al PNAS(107) 2010, [3] Yacoub E. et al NI(24) 2005, [4] Yacoub E. et al MRM(49) 2003, [5] Petridou N. et al, ISMRM 18th Scientific Meeting 2010 Proc.;3849,[6] Smith SM. HBM(17) 2002, [7] Hagberg GE. et al. NI(14) 2001, [8] Cox RW. CBR(29) 1996, [9] Glover GH. et al MRM(44) 2000, [10] Smith SM. et al NI(23) 2004, [11] Ari N. et al IEEE/EMBS proc. 2001